Monthly Notices
of the
ROYAL ASTRONOMICAL SOCIETY

MNRAS **438,** 2–13 (2014) doi:10.1093/mnras/stt1492
Advance Access publication 2013 December 21

Ultraviolet-excess sources with a red/infrared counterpart: low-mass companions, debris discs and QSO selection

Kars Verbeek,[1★] Paul J. Groot,[1] Simone Scaringi,[1,2] Jorge Casares,[3] Jesus M. Corral-Santana,[3,4] Niall Deacon,[5] Janet E. Drew,[6] Boris T. Gänsicke,[7] Eduardo González-Solares,[8] Robert Greimel,[9] Ulrich Heber,[10] Ralf Napiwotzki,[6] Roy H. Østensen,[2] Danny Steeghs,[7] Nicholas J. Wright[6] and Albert Zijlstra[11]

[1]*Department of Astrophysics, Radboud University Nijmegen, PO Box 9010, NL-6500 GL Nijmegen, the Netherlands*
[2]*Instituut voor Sterrenkunde, KU Leuven, Celestijnenlaan 200D, B-3001 Leuven, Belgium*
[3]*Instituto de Astrofísica de Canarias, Via Lactea s/n, E-38205 La Laguna (Tenerife), Spain*
[4]*Departamento de Astrofísica, Universidad de La Laguna, E-38205 La Laguna (Tenerife), Spain*
[5]*Max-Planck-Institute für Astronomie, Königstuhl 17, D-69117 Heidelberg, Germany*
[6]*Centre for Astronomy Research, Science & Technology Research Institute, University of Hertfordshire, Hatfield AL10 9AB, UK*
[7]*Physics Department, University of Warwick, Coventry CV4 7AL, UK*
[8]*Cambridge Astronomy Survey Unit, Institute of Astronomy, University of Cambridge, Madingley Road, Cambridge CB3 0HA, UK*
[9]*Institut für Physik, Karl-Franzen Universität Graz, Universitätsplatz 5, A-8010 Graz, Austria*
[10]*Dr. Remeis-Sternwarte Bamberg, Universität Erlangen-Nürnberg, Sternwartstrasse 7, D-96049 Bamberg, Germany*
[11]*Jodrell Bank Centre for Astrophysics, Alan Turing Building, University of Manchester, Manchester M13 9PL, UK*

Accepted 2013 August 6. Received 2013 August 5; in original form 2013 April 29

ABSTRACT

We present the result of the cross-matching between ultraviolet (UV)-excess sources selected from the UV-Excess Survey of the Northern Galactic Plane (UVEX) and several infrared (IR) surveys (2MASS, UKIDSS and *WISE*). From the position in the $(J - H)$ versus $(H - K)$ colour–colour diagram, we select UV-excess candidate white dwarfs with an M-dwarf type companion, candidates that might have a lower mass, brown-dwarf type companion and candidates showing an IR-excess only in the K band, which might be due to a debris disc. Grids of reddened DA+dM and sdO+MS/sdB+MS model spectra are fitted to the U, g, r, i, z, J, H, K photometry in order to determine spectral types and estimate temperatures and reddening. From a sample of 964 hot candidate white dwarfs with $(g - r) < 0.2$, the spectral energy distribution fitting shows that ∼2–4 per cent of the white dwarfs have an M-dwarf companion, ∼2 per cent have a lower-mass companion, and no clear candidates for having a debris disc are found. Additionally, from *WISE* six UV-excess sources are selected as candidate quasi-stellar objects (QSOs). Two UV-excess sources have a *WISE* IR-excess showing up only in the mid-IR $W3$ band of *WISE*, making them candidate luminous infrared galaxies (LIRGs) or Sbc starburst galaxies.

Key words: surveys – binaries: general – white dwarfs – ISM: general – Galaxy: stellar content – infrared: stars.

1 INTRODUCTION

One of the main goals of the European Galactic Plane Surveys (EGAPS) is to obtain a homogeneous sample of evolved objects in our Milky Way with well-known selection limits. The EGAPS data also contain more esoteric objects (e.g. Nova V458 Vul, Wesson et al. 2008; Necklace Nebula, Corradi et al. 2011; photo-evaporating prolyd-like objects, Wright et al. 2012). Over the past years the data of large sky surveys yielded several known white dwarfs with gas or dust discs (Zuckerman & Becklin 1987; Gänsicke, Marsh & Southworth 2007; Gänsicke et al. 2008; Brinkworth et al. 2009; Debes et al. 2011a,b; Gänsicke 2011; Brinkworth et al. 2012; Kilic et al. 2012). When optical surveys are cross-matched with the data of infrared (IR) surveys (e.g. SDSS-UKIDSS: Silvestri et al. 2006; Heller et al. 2009; Girven et al. 2011, SDSS-*WISE*: Debes et al. 2011b; Hoard et al. 2011, SDSS-2MASS: Hoard et al. 2011 and IPHAS-2MASS: Wright et al. 2008), the classification of sources can be extended, and hot white dwarfs with companions or debris discs, and other peculiar objects are detected. The dusty debris discs

★ E-mail: k.verbeek@astro.ru.nl

around white dwarfs are believed to form during the destruction of asteroids, the remnants of the planetary systems that orbited the star earlier in its evolution at the main sequence. Emission lines in the spectra of the white dwarfs indicates that there might also be gaseous material present in these discs. This might also clarify the spectra of metal-polluted white dwarfs (Debes & Sigurdsson 2002; Jura 2003; Debes, Walsh & Stark 2012; Dufour et al. 2012; Farihi et al. 2012; Gänsicke et al. 2012). The time for metals to sink out of the atmosphere of the white dwarf is in the order of a few days for hot DA white dwarfs, and up to 10^6 years for DB/DC white dwarfs (tables 4–6 of Koester 2009; Koester & Wilken 2006), indicating that accretion is ongoing for most objects. An unknown fraction of the UV-Excess Survey of the Northern Galactic Plane (UVEX) white dwarfs will have an M-dwarf companion (Farihi, Becklin & Zuckerman 2005; Silvestri et al. 2006; Debes et al. 2011b). From the cross-matching between IR and optical observations, about 0.2–2 per cent of the white dwarfs are expected to have an IR-excess due to a brown-dwarf type companion, and 0.3–4 per cent of the white dwarfs are expected to be debris disc candidates (Farihi et al. 2005; Debes et al. 2011b; Girven et al. 2011; Steele et al. 2011; Barber et al. 2012).

A number of the optically selected ultraviolet (UV)-excess sources from UVEX, as described in Verbeek et al. (2012a, hereafter V12a), will show a near-IR (NIR) and mid-IR (MIR) excess due to a low-mass companion or due to interstellar and/or circumstellar material. The UV-excess catalogue of V12a consists of a mix of different populations, such as white dwarfs, interacting white dwarf binaries, subdwarfs of type O and B (sdO/sdB), emission-line stars and quasi-stellar objects (QSOs). Due to the limited statistics and inhomogeneity, the fraction of optically selected white dwarfs with an IR-excess due to a low-mass companion is very uncertain in the Galactic Plane (Hoard et al. 2011). The UV-excess catalogue of V12a offers a complete white dwarf sample for this purpose, even though the sample also contains other populations. A distinction between white dwarfs with a companion or disc and e.g. young stellar objects (YSOs), Be stars and cataclysmic variables can be made using the strength of the Hα emission (Witham et al. 2008; Corradi et al. 2010; Barentsen et al. 2011). A fraction of the subdwarf stars and A-type stars in the UV-excess catalogue might show an IR excess (Hales et al. 2009), and UV-excess sources can also have both an optical blueness and IR excess when they are non-stellar, e.g. QSOs (Wright et al. 2008; Roseboom et al. 2013; Xue-Bing et al. 2013).

The UVEX survey images a $10 \times 185^\circ$ wide band ($-5^\circ < b < +5^\circ$) centred on the Galactic equator in the U, g, r and He I λ5875 bands down to ∼21–22 mag using the Wide Field Camera mounted on the Isaac Newton Telescope on La Palma (Groot et al. 2009). From the first 211deg^2 of UVEX data a catalogue of 2 170 UV-excess sources was selected in V12a. These UV-excess candidates were selected from the $(U - g)$ versus $(g - r)$ colour–colour diagram and g versus $(U - g)$ and g versus $(g - r)$ colour–magnitude diagrams by an automated field-to-field selection algorithm. Less than ∼1 per cent of these selected UVEX sources are known in the literature. Spectroscopic follow-up of 132 UV-excess candidates selected from UVEX, presented in Verbeek et al. (2012b, hereafter V12b), shows that most UV-excess candidates are indeed genuine UV-excess sources such as white dwarfs, subdwarfs and interacting white dwarf binaries.

In this work we present the IR photometry of the UV-excess sources in the UVEX catalogues of V12a. Our goals are (i) to see what fraction of the hot white dwarfs have a companion (late MS or BD), (ii) to see if we can use IR photometry to select non-white dwarfs from our UV-excess catalogue and iii) to see if we can find any debris discs. In Section 2, the cross-matching of the full UV-excess catalogue with IR/red surveys is presented. In Section 3, hot UV-excess candidate white dwarfs with $(g - r) < 0.2$ with an IR-excess are selected and classified by fitting grids of reddened DA+dM and sdO/sdB models to the optical and IR photometry. The spectral types of companions later than M6 are determined from the IR-excess. From these results the fraction of hot white dwarfs with a low-mass companion is derived. In Section 4, the matches of the UV-excess sources in the *Wide-field Infrared Survey Explorer* (*WISE*) data are presented, and additionally a list of candidate QSOs with $|b| < 5^\circ$ is selected. Finally in Section 5, we summarize and discuss the conclusions.

Table 1. Summary of the cross-matching: No. of matches with the full UV-excess catalogue and No. of matches in the Deacon PM/Witham Hα catalogues (Witham et al. 2008; Deacon et al. 2009).

Catalogue:	Full UV-excess	PM/Hα
UKIDSS-GPS	227	4/6
2MASS	60	2/5
WISE	19	1/2
IPHAS-IDR	1203	26/15
SDSS DR8	378	6/3

2 CROSS-MATCHING WITH IR SURVEYS: UKIDSS, 2MASS AND *WISE*

The UV-excess catalogue of V12a (2 170 sources) is cross-matched with different surveys that image (parts of) the Galactic Plane at red/IR wavelengths. An overview of the cross-matching is given in Table 1. Note that the coverage of the Galactic Plane and the overlap with the UVEX fields of V12a are not complete for all surveys (see Section 5). The results of the cross-matching are shown in the colour–colour diagrams of Fig. 1–5, where the spectroscopically classified sources of V12b are labelled. The UKIRT InfraRed Deep Sky Survey (UKIDSS) and Two Micron All Sky Survey (2MASS) colour–magnitude diagrams are shown in Appendix A. As expected, in particular the redder and brighter UVEX UV-excess sources have a larger fraction of IR matches, as can be seen in the UVEX colour–colour and colour–magnitude diagrams of Fig. 1 and 2. The different IR surveys and the number of matches with the full UV-excess catalogue of V12a are described below.

(i) The UKIDSS (Lawrence et al. 2007) is an NIR survey imaging the northern sky in the J, H and K (1.2, 1.6 and 2.2µm) filters using the Wide Field Camera (WFCAM) mounted on the 3.8-m United Kingdom Infrared Telescope (UKIRT) on Hawaii. The UKIDSS Galactic Plane Survey (UKIDSS-GPS; Lucas et al. 2008; Lawrence et al. 2012) images the northern Galactic Plane in the same Galactic latitude range as UVEX and INT/WFC Photometric Hα Survey of the Northern Galactic Plane (IPHAS). There is a match for a total of 227 UV-excess sources in all three UKIDSS filters within a radius of 1 arcsec (10 per cent of the complete UV-excess catalogue). Note that the overlap of the UKIDSS-GPS Data Release 1 (DR1) with the UVEX fields of V12a is not complete. The UV-excess three-filter matches in UKIDSS with $K > 11$ are plotted in the colour–colour diagram of Fig. 3 on top of the simulated unreddened main-sequence colours (Hewett et al. 2006). Of these UKIDSS matches, there are

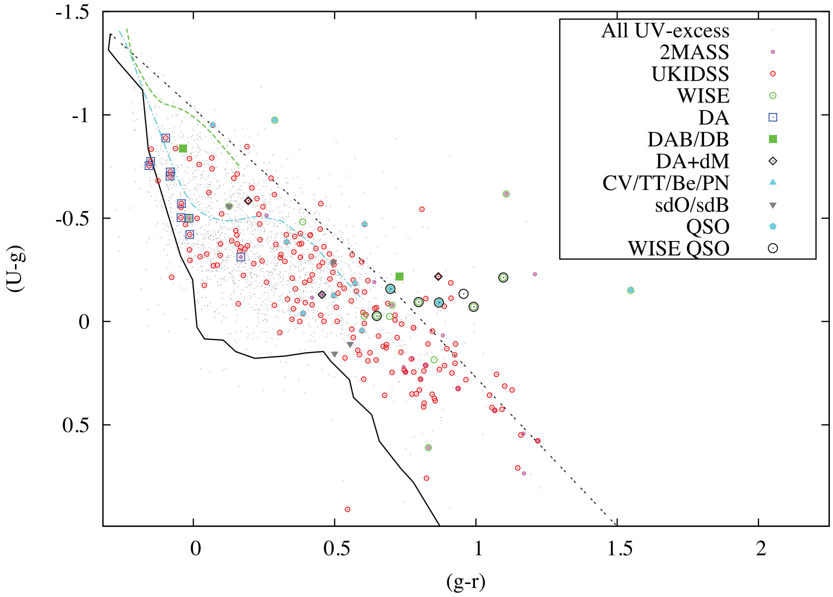

Figure 1. Colour–colour diagram with the UV-excess matches in UKIDSS, 2MASS and *WISE*. UV-excess sources spectroscopically classified in V12b are overplotted with different symbols. The lines are the simulated colours of unreddened main-sequence stars (solid black) and the O5V-reddening line (dashed black) of V12a. The cyan and green dashed lines are, respectively, the simulated colours of unreddened Koester DA and DB white dwarfs. The grey dots are the sources from the complete UV-excess catalogue of V12a.

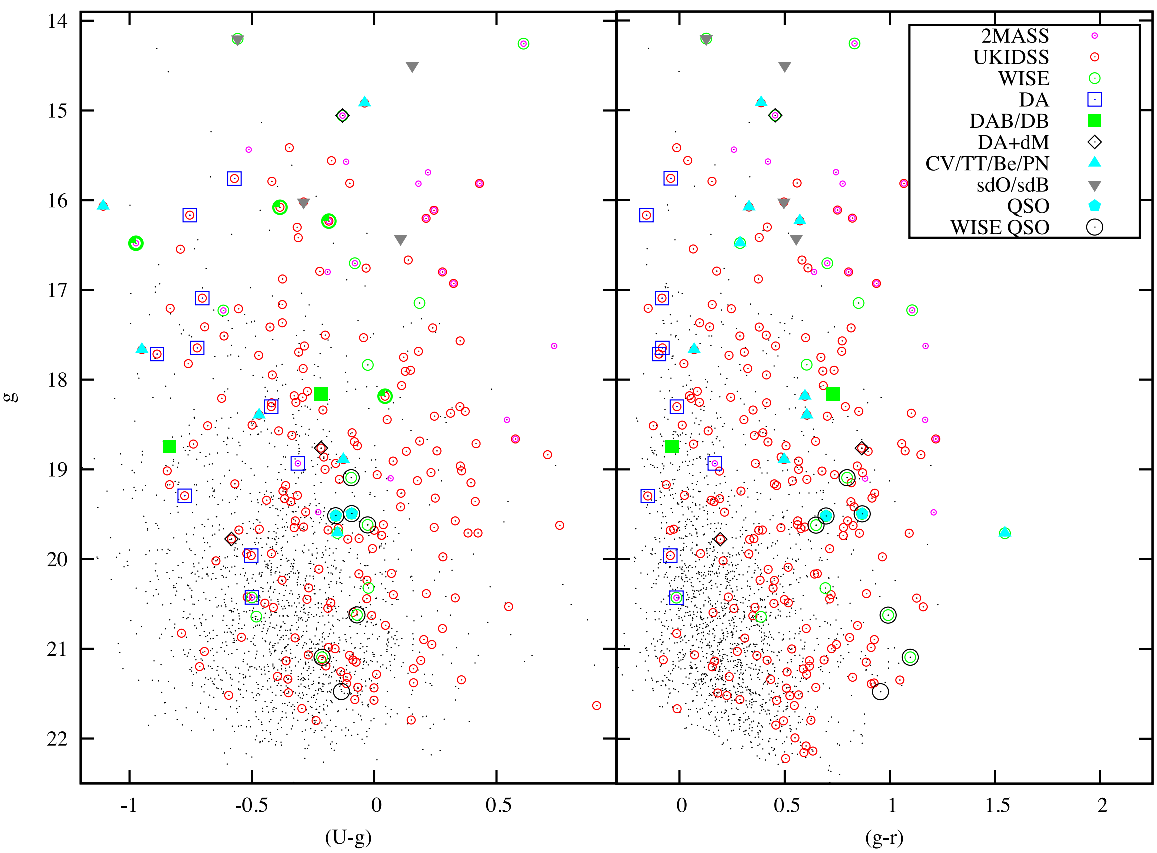

Figure 2. Colour–magnitude diagrams with the UV-excess matches in UKIDSS, 2MASS and *WISE*. Spectroscopically identified UV-excess sources of V12b are overplotted with different symbols. The grey dots are the sources from the complete UV-excess catalogue of V12a.

18 sources spectroscopically classified in V12b, four matches are in the IPHAS-POSSI proper motion (PM) catalogue (Deacon et al. 2009) and six matches are in the Hα emitter catalogue (Witham et al. 2008).

(ii) The 2MASS (Cutri et al. 2003; Skrutskie et al. 2006) imaged the entire sky in the three NIR filter bands J, H and K (1.2, 1.7 and 2.2µm) with a limiting magnitude of $J = 17.1$, $H = 16.4$ and $K = 15.3$, using two automated 1.3 m telescopes: one at Mt. Hopkins,

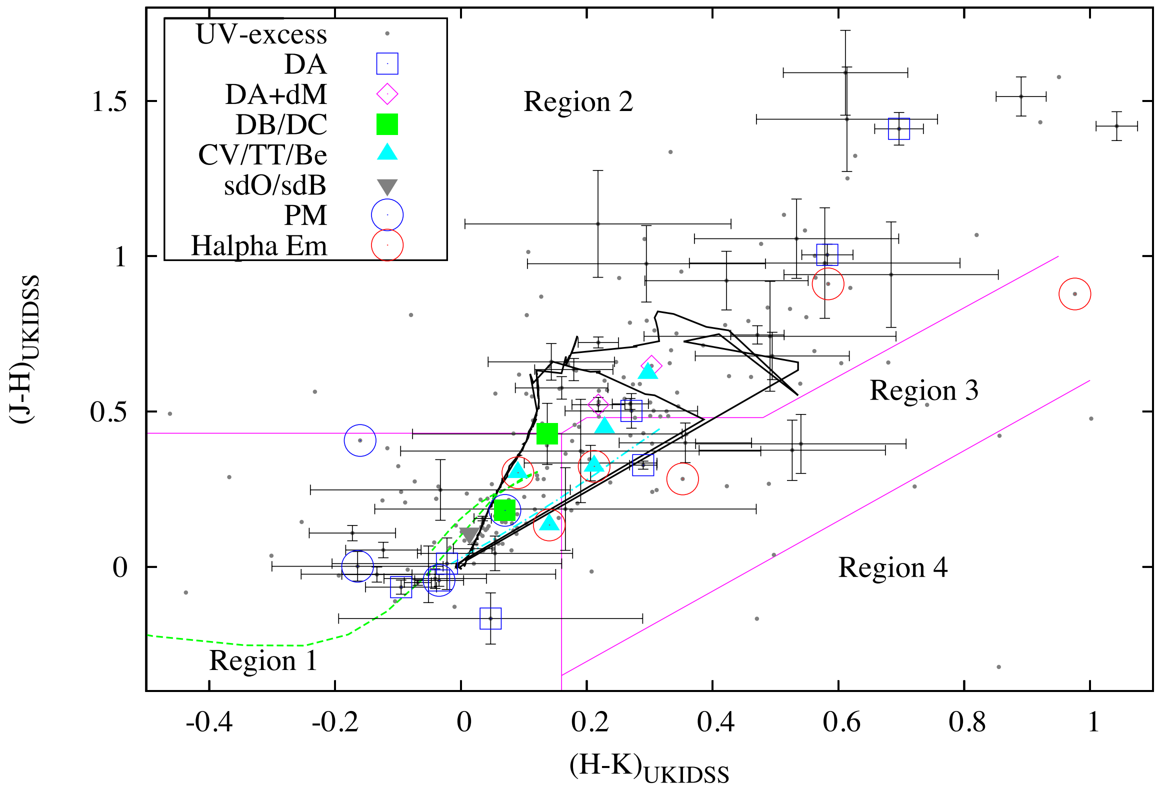

Figure 3. The $(J-H)$ versus $(H-K)$ colour–colour diagram with the UKIDSS-GPS matches. The tracks are the unreddened UKIDSS colours of main-sequence stars (black), DA white dwarfs (green) and DB white dwarfs (cyan). UV-excess sources spectroscopically classified in V12b are overplotted with different symbols, UV-excess candidate white dwarfs with $(g-r) < 0.2$ are plotted with error bars and other UV-excess sources are plotted with dots. The four regions are indicated that contain different candidates: (1) single white dwarfs, (2) white dwarfs with an M-dwarf companion, (3) candidate white dwarfs with a later type (brown dwarf) companion and (4) white dwarf with circumstellar material or a debris disc.

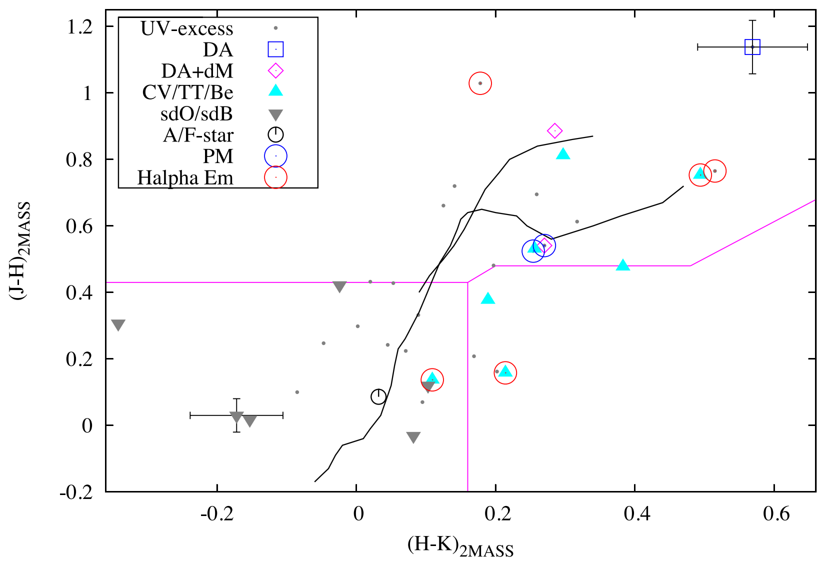

Figure 4. $(J-H)$ versus $(H-K)$ colour–colour diagram with the UV-excess matches in 2MASS. The black lines are the simulated colours of main-sequence stars and giants with $E(B-V) = 0$. Classified sources are labelled with different symbols, UV-excess candidate white dwarfs are plotted with error bars and other UV-excess sources are plotted with dots. There is one more match at $(H-K) = 1.15$, $(J-H) = 2.6$, classified as DA white dwarf in V12b, not visible in this figure.

Arizona, and one at CTIO, Chile. The overlap of the 2MASS All-Sky Catalog of Point Sources (Cutri et al. 2003) data and the UVEX fields of V12a is 100 per cent. In 2MASS there is a match for 60 sources of the complete UV-excess catalogue in all three 2MASS filter bands within a radius of 1 arcsec (3 per cent). Eighteen of these matches were spectroscopically classified in V12b, 2 matches are the IPHAS-POSSI catalogue (1 classified as DA+dM) and 5 matches are in the Hα emitter catalogue (3 classified as T Tauri, Be

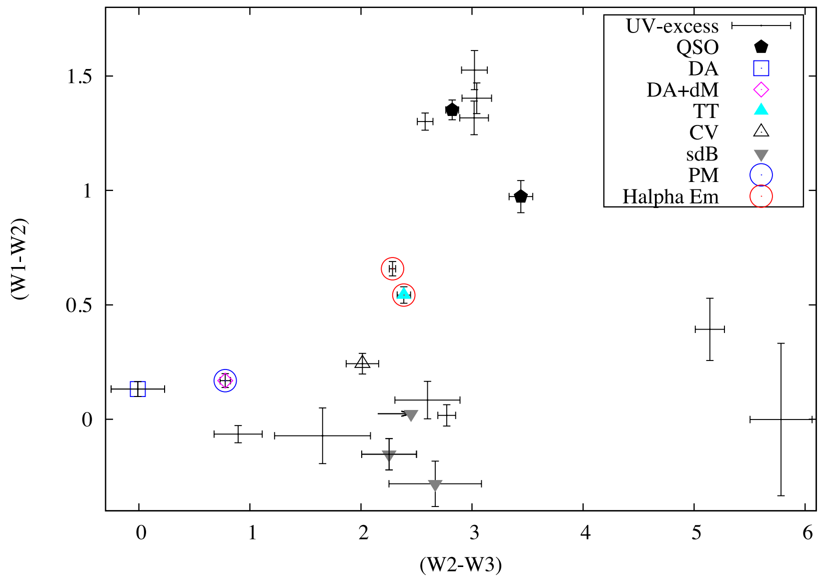

Figure 5. *WISE* matches within 1 arcsec plotted in the *WISE* colour–colour diagram. Sources which are classified from their spectra in V12b are overplotted with different symbols and all UV-excess matches are plotted with error bars. The 2 sources at $(W2-W3)=0$ and $(W2-W3)=5.8$ are UV-excess candidate white dwarfs with $(g-r)<0.2$, 1 classified as DA white dwarf in V12b and 1 unclassified source with a strong $W3$ excess and $(W3-W4)=2.1$.

star and cataclysmic variable). The UV-excess matches in 2MASS are plotted in the colour–colour diagram of Fig. 4.

(iii) The *WISE* (Wright et al. 2008) mapped the sky at four MIR bands at 3.4, 4.6, 12 and 22 µm ($W1$, $W2$, $W3$ and $W4$). The overlap of the *WISE* All-Sky Data Release (Cutri et al. 2012) and the UVEX fields of V12a is 100 per cent. The *WISE* data are used to select and classify UV-excess sources with a mid-IR excess, and a list of UV-excess candidate QSOs is selected in Section 4. There is a match for 20 UV-excess sources in *WISE* within a radius of 1 arcsec in at least the first three filters ($W1$, $W2$, $W3$). Thirteen of them have a match in all four *WISE* filters. The three-filter matches are shown in the colour–colour diagram of Fig. 5.

(iv) The IPHAS (Drew et al. 2005) has imaged the same survey area as UVEX with the same telescope and camera set-up using the r, i and Hα filters. There is a match for 1 203 of our 2 170 UV-excess sources in the IPHAS initial data release (IDR; González-Solares et al. 2008) within a radius of 1.0 arcsec (55 per cent). Note that the overlap of the IPHAS IDR with the UVEX fields of V12a is not complete, but ∼90 per cent. The result of the cross-match between the UV-excess catalogue and IPHAS IDR was already shown in figs 10 and 11 of V12a and fig. 3 of V12b. If available, the IPHAS data are used to distinguish UV-excess white dwarfs from UV-excess sources showing Hα emission, and the i-band photometry is used in the spectral fitting in Section 3.2. In the colour–colour diagrams of Fig. 3–5, the sources that are in the IPHAS Hα emitter catalogue (Witham et al. 2008) or IPHAS-POSSI PM catalogue (Deacon et al. 2009) are circled red and blue, respectively. The Witham Hα emitter catalogue covers the magnitude range $13<r<19.5$ and the Deacon IPHAS-POSSI PM catalogue covers the magnitude range $13.5<r<19$. Matches in the Hα emission line star catalogue are expected to be Galactic sources, except for QSOs with redshift 0.5 or 1.3, which have emission lines exactly in the bandpass of the IPHAS Hα filter (Scaringi et al. 2013).

(v) Additionally, the Sloan Digital Sky Survey (SDSS; York et al. 2000) Photometric Catalog DR8 (Adelman-McCarthy et al. 2011) overlaps with some UVEX Galactic Plane fields. SDSS images the sky in the filters u, g, r, i, z down to ∼22 mag, using the 2.5 m wide-angle optical telescope at Apache Point Observatory, New Mexico, US. For the full UV-excess catalogue 378 sources have a match in SDSS within a radius of 1 arcsec. Note that the overlap between SDSS and the UVEX fields of V12a is not complete. There are six SDSS UV-excess matches in the IPHAS-POSSI PM catalogue and three SDSS UV-excess matches are in the IPHAS Hα emitter catalogue. For the UV-excess sources that have an SDSS match, the additional i-band and z-band photometry is used for the spectral fitting (fig. 1, Rebassa-Mansergas et al. 2012) in Section 3.2.

3 CANDIDATE WHITE DWARFS WITH AN INFRARED COUNTERPART

The UV-excess catalogue consists of a mix of different populations. From the spectroscopic follow-up of V12b, 52 per cent of the UV-excess sources are single DA white dwarfs, 14 per cent are white dwarfs of other types (DAB/DB/DC/DZ/DAe), 4 per cent are DA+dM white dwarfs, 11 per cent are sdB/sdO stars, 9 per cent are Hα emission line objects, 8 per cent are BHB/MS stars and 2 per cent are QSO. In Sections 3.1 and 3.2 we focus in particular on hot white dwarfs with an IR match. For that reason a sub-sample of 964 UV-excess candidate white dwarfs with $(g-r)<0.2$ is selected, which corresponds with the simulated unreddened colours of DA white dwarfs hotter than $T_{\rm eff}>9000$ K. This sub-sample does not contain DA white dwarfs cooler than $T_{\rm eff}<9000$ K or strongly reddened white dwarfs. From spectroscopic follow-up (fig. 1, V12b) it is known that 97 per cent of the DA white dwarfs identified in UVEX are in this colour range, but there will be ∼25 per cent white dwarfs of other types and sdO/sdB stars which also may have IR counterparts. Only the IR matches of the sources from this UV-excess candidate white dwarf sub-sample are plotted with error bars in the colour–colour diagrams of Fig. 3–5.

3.1 Classification of white dwarfs in UKIDSS and 2MASS

In the hot sub-sample there are 46 UV-excess candidate white dwarfs with a UKIDSS match, and 3 with a 2MASS match. These matches are plotted with error bars in the colour–colour diagrams of Fig. 3 and 4. To separate single white dwarfs from white dwarfs with a companion or white dwarfs with a debris disc the $(J - H)$ versus $(H - K)$ colour–colour diagram is divided into four separate regions following Wachter et al. (2003) and Steele et al. (2011). The different regions in Fig. 3 contain different candidates.

(i) Region 1: there are 17 UV-excess sources that are single candidate white dwarfs, of which 4 were already classified as hydrogen atmosphere (DA) white dwarfs and 1 classified as sdB star in V12b.

(ii) Region 2: sources in region 2 are candidates for white dwarfs with an M-dwarf companion. There are 22 UV-excess candidates, of which 11 have $g < 20$. Five of these sources are classified as single DA white dwarfs in V12b. However, the available spectra cannot exclude the presence of a late-type companion.

(iii) Region 3: sources in region 3 are candidates for white dwarfs with a later-type (brown dwarf) companion. There are seven UV-excess candidate white dwarfs, one of them is classified as a DA white dwarf in V12b (UVEXJ202659.21+411644.1). The available spectrum cannot exclude the presence of a very late-type companion.

(iv) Region 4: sources in region 4 show a K-band excess, possibly due to circumstellar material or a disc. There are five UV-excess sources, but none of them are candidate hot white dwarfs since they have $(g - r) > 0.2$ in UVEX.

3.2 Determination of spectral types

For the UV-excess candidate white dwarfs with an IR-excess match in UKIDSS and/or 2MASS, the spectral energy distributions (SEDs) are fitted in order to determine the spectral types. Grids of DA+dM model spectra, in the range of $0 < E(B - V) < 1.0$ at $E(B - V) = 0.1$ intervals, using the reddening laws of Cardelli, Clayton & Mathis (1989), are fitted to the optical and IR photometry in order to determine white dwarf temperatures. For the fitting the white dwarf atmosphere models and M-dwarf models are both placed at the same distance. The spectral fluxes of Beuermann (2006) are used to calibrate the absolute fluxes of the M dwarfs. The grid of DA+dM model spectra is constructed from white dwarf atmosphere model spectra of Koester et al. (2001) with $\log g = 8.0$ in the range $6000 < T_{\rm eff} < 80\,000$ K, and template spectra of main-sequence stars from the library of Pickles (1998) with spectral type M0V–M6V. First, the UVEX photometry is used to determine the temperature of the white dwarf. For the DA+dM SED fitting the photometry of UVEX, UKIDSS and 2MASS, and additionally if available, the IPHAS and/or SDSS photometry, is used for 40 candidate white dwarfs. The *WISE* photometry is not used since the wavelength range of the DA+dM models only covers 3000–25 000 Å, but consistency with the *WISE* photometry was checked, see e.g. Fig. 7.

The DA+dM models do not give a good fitting result for all candidate white dwarfs with an IR-excess match. Some UV-excess sources with an IR-excess match can be fully explained by a reddened sdB or sdO spectrum without any companion, or the IR-excess can be explained by an sdB/sdO stars with an F-, G- or K-type main-sequence companion. SdB/sdO stars with later companions cannot be identified with the current photometry because the sdB/sdO dominates the SED out to the K band. Grids of TheoSSA (Ringat 2012) sdB/sdO models with $\log g = 5.5$ in the range $20\,000 < T_{\rm eff} < 50\,000$ K and $0 < E(B - V) < 5.0$ at $T_{\rm eff} = 1000$ K and $E(B - V) = 0.1$ intervals are fitted to the optical and IR photometry to determine $T_{\rm eff}$ and the reddening of the sdB/sdO stars. For the sdO/sdB stars with a possible main-sequence companion, a grid is constructed from the reddened sdB/sdO models and the template spectra of main-sequence stars from the library of Pickles (1998) with spectral types A5V–M5V. Also here the *WISE* photometry is not used, but consistency was checked, since the sdO/sdB+MS models cover the wavelength range 3000–25 000 Å.

Candidate white dwarfs in region 3 of the IR colour–colour diagrams have companions with spectral types later than M6. The spectral types of these companions are determined using the $(J - K)$ colours resulting after subtracting the white dwarf flux as explained in Reid et al. (2001) and Leggett et al. (2002). The UKIDSS colours are converted to AB colours taking into account the correction $(J - K) = 0.962$ of Hewett et al. (2006).

In the original UV-excess catalogue there might be a possible systematic shift in the UVEX U-band data, which would influence the result of SED fitting in this paper. For that reason recalibrated UVEX data, as explained in Greiss et al. (2012), is used. The shift in the original UVEX data does not influence the content of the UV-excess catalogue because the selection in V12a was done relative to the reddened main-sequence population. The magnitudes and colours of the UV-excess sources might still show a small scatter, similar to the early IPHAS data (Drew et al. 2005), since a global photometric calibration is not applied to the UVEX data.

To convert the magnitudes into fluxes (F) we use: $F = 10^{-0.4\times(\mathrm{mag_{(AB)}}+48.6)}$ for EGAPS and SDSS. For EGAPS, photometry the AB offsets $U = 0.927$, $g = -0.103$, $r = 0.164$ and $i = 0.413$ need to be added to convert to AB magnitudes (Hewett et al. 2006; Blanton & Roweis 2007; González-Solares et al. 2008). To convert UKIDSS photometry to AB magnitudes the correction $J = 0.938$, $H = 1.379$ and $K = 1.900$ need to be taken into account (Hewett et al. 2006). For 2MASS the flux is derived using $F = F_{\nu} - 0\,\mathrm{mag} \times 10^{-0.4\times(\mathrm{mag_{(Vega)}})}$, where $F_{\nu} - 0\,\mathrm{mag}$ is 1594, 1024 and 666,7 (Jy) for J, H and K, respectively (Cutri et al. 2003). The *WISE* photometry is converted into fluxes using $F = F_{\nu 0} \times 10^{-0.4\times \mathrm{mag_{(Vega)}}}$, where $F_{\nu 0}$ is the 'Zero Magnitude Flux Density' for the *WISE* filter bands: $W1 = 309.54$, $W2 = 171.787$, $W3 = 12.82$ and $W4 = 9.26$ (Jy) (Wright et al. 2008).

3.3 Fitting results

To test our photometric fitting routine first the method is applied to the UV-excess candidate white dwarfs that were spectroscopically classified in V12b. Note that the aim of the fitting is not to derive accurate temperatures, spectral types and reddening, but to classify the sources, and to confirm (or to rule out) the presence of a companion or disc. Fitting results for 7 UV-excess sources, spectroscopically classified in V12b, with an IR-excess or just an IR match, are shown in Fig. 6–12. For some of these sources there is also a match in *WISE* (see Section 3.4).

(i) The object UVEXJ1909+0213, classified as DA+dM objects in V12b, is shown in Fig. 6. This source has $(g - r) = 0.87$, so it is not in the UV-excess candidate white dwarf sub-sample. The best-fitting model consists of a white dwarf with $T_{\rm eff} = 14$ kK with an M4V companion. This source is in region 2 of the 2MASS colour–colour diagram of Fig. 4 and in region 2 of the UKIDSS colour–colour diagram of Fig. 3. Note that only the photometry was used for the fitting.

(ii) The object UVEXJ2122+5526, also classified as DA+dM objects in V12b, is shown in Fig. 7. This source has $(g - r) = 0.47$, so it is also not in the UV-excess candidate white dwarf sub-sample. The model that fits best consists of a white dwarf with $T_{\rm eff} = 20$ kK with an M3V companion, which is consistent up to the $W3$ *WISE* photometry. This source is in region 2 of the 2MASS colour–colour diagram of Fig. 4 and is plotted in the *WISE* colour–colour diagram of Fig. 5.

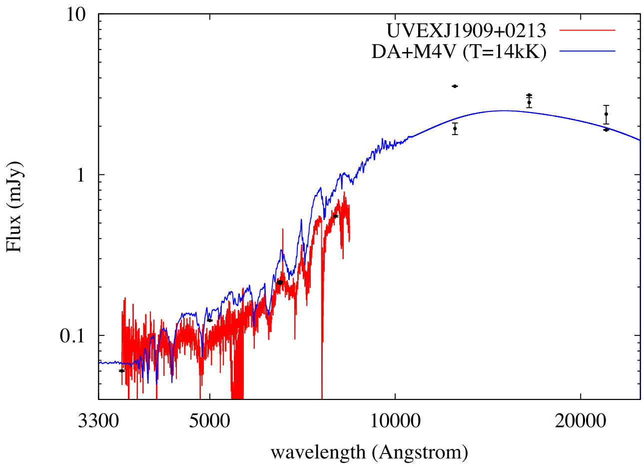

Figure 6. The SED of UVEXJ190912.34+021342.8, classified as DA+dM in V12b, with overplotted the best DA+dM model (blue), a $T_{\rm eff} = 14$ kK white dwarf plus M4V companion. Plotted here are the UVEX, IPHAS, 2MASS and UKIDSS photometry with error bars and the WHT spectrum of V12b (red).

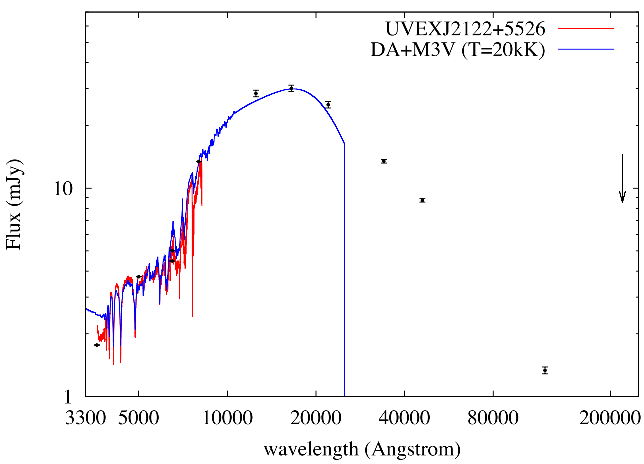

Figure 7. The SED of UVEXJ212257.82+552609.0, classified as DA+dM in V12b, can indeed be explained by DA+dM model (blue): a $T_{\rm eff} = 20$ kK white dwarf plus M3V companion, except for the W4 *WISE* photometry which is spurious. Plotted here are the UVEX, IPHAS, 2MASS and *WISE* photometry with error bars and the WHT spectrum of V12b (red).

(iii) The SED of UVEXJ2239+5857, classified as He-sdO in V12b, shows a decreasing flux in the IR which can be explained with a reddened sdB/sdO spectrum with $T_{\rm eff} = 50$ kK, $\log g = 5.5$ and $E(B-V) = 0.8$, which is the model that fits best for this object, see Fig. 8.

(iv) The SED of UVEXJ0421+4651, classified as sdB+F in V12b, can be explained by a single reddened sdB/sdO spectrum, but the combination of a sdB and a K5V spectrum gives a slightly better fit with $T_{\rm eff} = 50$ kK, $E(B-V) = 1.0$, see Fig. 9. This source was classified as sdB+F in V12b due to the CaII lines present in the optical spectrum.

(v) The photometry of UVEXJ0328+5035, classified as a sdB star in V12b, can be fully explained by a reddened sdB spectrum with $T_{\rm eff} = 30$ kK, $\log g = 5.5$ and $E(B-V) = 0.4$, see Fig. 10. However, this object is known to be a sdB+dM binary from its radial velocity (Kupfer et al. 2013). No sign of the companion is seen in the SED.

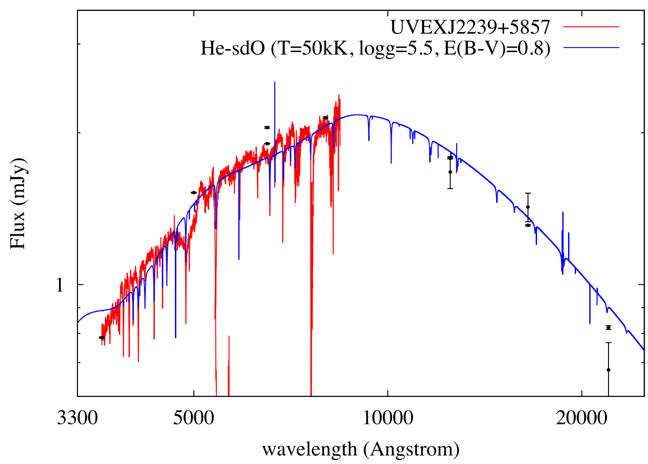

Figure 8. The photometry of UVEXJ223941.98+585729.1, classified as He-sdO in V12b, can be fully explained by a reddened He-sdO spectrum with $T_{\rm eff} = 50$ kK, $\log(g) = 5.5$ and $E(B-V) = 0.8$ (blue). Plotted here are the UVEX, IPHAS, UKIDSS and 2MASS photometry with error bars and the WHT spectrum of V12b (red).

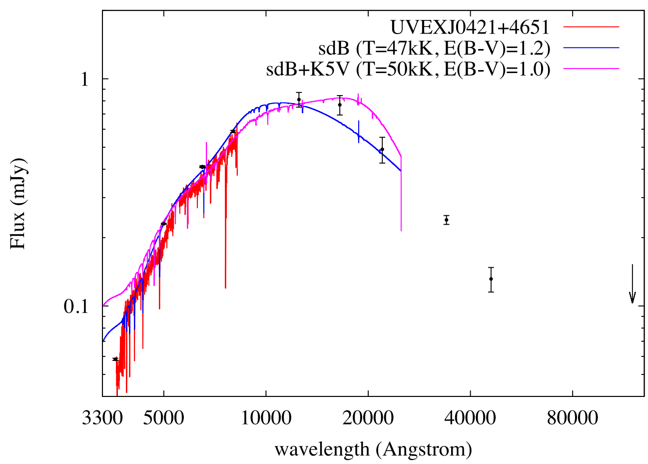

Figure 9. The photometry of UVEXJ042125.70+465115.4, classified as sdB+F in V12b, overplotted with a single sdB spectrum with $T_{\rm eff} = 47$ kK, $E(B-V) = 1.2$ (blue), and the best-fitting sdB+MS model: a sdB+K5V spectrum with $T_{\rm eff} = 50$ kK, $E(B-V) = 1.0$ (magenta). Plotted here are the UVEX, IPHAS, 2MASS and *WISE* photometry with error bars and the WHT spectrum of V12b (red).

(vi) The SED fitting method finds a DA+dM as best solution for source UVEXJ2034+4110 (Fig. 11), classified as a DA white dwarf in V12b. The best-fitting DA+dM model is a $T_{\rm eff} = 13$ kK DA white dwarf plus an M6V companion. The strong IR-excess is due to a low-mass companion with spectral type L8 as determined from the $(J-K)$ colour. However, the contribution of an low-mass companion with spectral type L8 would be less luminous than in Fig. 11, so the white dwarf is probably at a larger distance compared to the brown dwarf. Additionally, the blue/optical images have a match within 0.1 arcsec, while there is an offset for the IR images of 0.6 arcsec. The white dwarf and L8 brown dwarf are expected to be at different distances and not physically associated.

(vii) The source UVEXJ2102+4750 in Fig. 12, classified as a DA white dwarf with $T_{\rm eff} = 13.3$ kK and $\log(g) = 8.1$ in V12b, shows an IR-excess. None of the DA+dM models fit the photometry well, making it candidate for having a companion with spectral type L5 as determined from the $(J-K)$ colour. This source was classified as

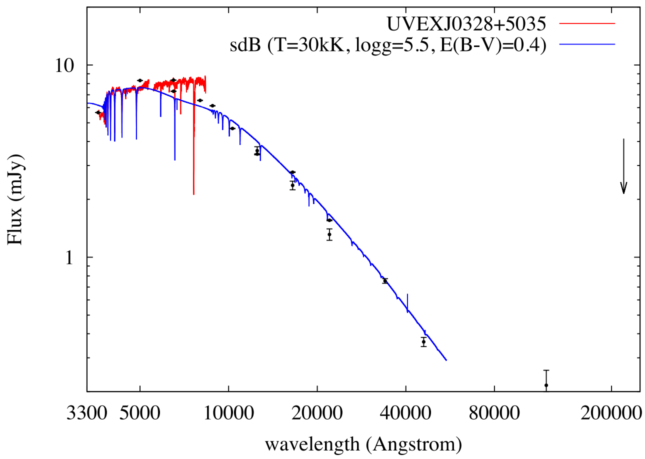

Figure 10. The photometry of UVEXJ032855.25+503529.8 can be fully explained by a reddened sdB model spectrum (blue) with $T_{\rm eff}$ = 30 kK, log (*g*) = 5.5 and $E(B-V)$ = 0.4. Plotted here are the UVEX, IPHAS, UKIDSS, 2MASS and *WISE* photometry with error bars and the WHT spectrum of V12b (red). The WHT spectrum might deviate at the red end of the spectrum (λ >7 500 Å) due to the flux calibration.

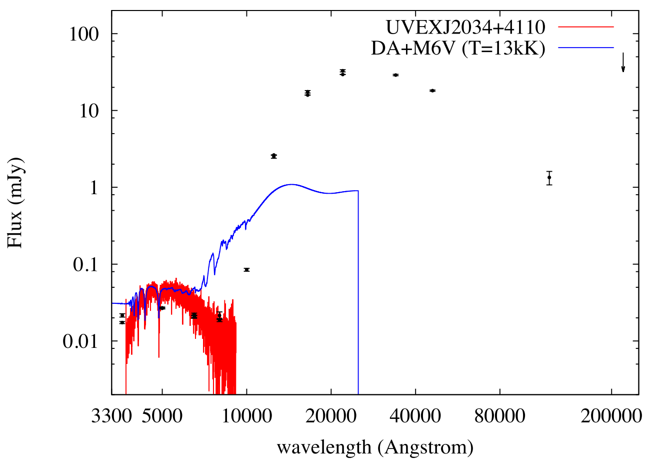

Figure 11. The SED of UVEXJ203411.72+411020.3, classified as single DA white dwarf in V12b, cannot be explained by one of our DA white dwarf plus a late type companion models. The best-fitting DA+dM model is a $T_{\rm eff}$ = 13 kK white dwarf plus M6V companion (blue). The strong infrared-excess in 2MASS, UKIDSS and *WISE* can be explained by a later companion with spectral type L8. However, the contribution of this L8 dwarf is significantly more luminous than expected, so the WD and BD are expected to be at different distances and not physically associated. Plotted here are the UVEX, IPHAS, SDSS, 2MASS, UKIDSS and *WISE* photometry with error bars and the Hectospec spectrum of V12b (red).

a DA white dwarf in V12b since there is no sign of the companion in the optical spectrum, which is consistent with the IR-excess which increases for wavelengths larger than λ > 8 000 Å.

The results of the fitting for all UV-excess candidate white dwarfs with an IR-excess match in UKIDSS and/or 2MASS are shown in Table A1. Note that $T_{\rm eff}$ of the white dwarf and the spectral types of the companions are rough estimates, since only photometry is used for the fitting. From the positions in the $(J-H)$ versus $(H-K)$ colour–colour diagram, and from the SED fitting, 24 UV-excess candidate white dwarfs are classified as white dwarf with an M-dwarf companion, 7 sources are candidate white dwarfs probably with a brown dwarf type companion (later than M type), 19 UV-excess candidate white dwarfs are single white dwarfs or single

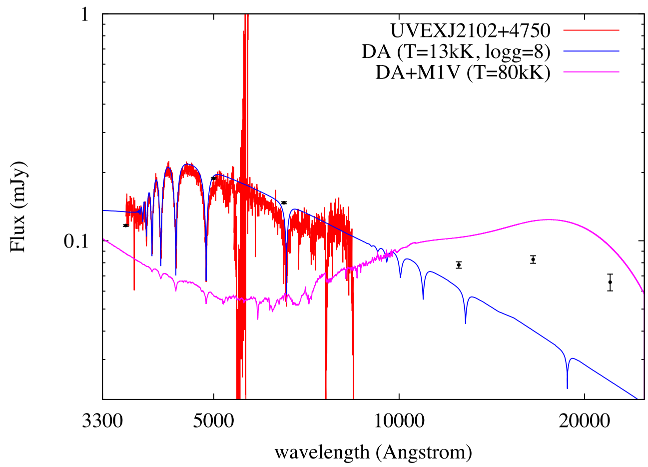

Figure 12. The SED of UVEXJ210248.44+475058.9, classified as DA white dwarf with $T_{\rm eff}$ = 13.3 kK and log (*g*) = 8.1 in V12b, shows a clear excess in the infrared which can be explained by a companion. The best-fitting DA+dM model is a $T_{\rm eff}$ = 80 kK white dwarf plus M1V companion (magenta), which is clearly too hot for the white dwarf. From the $(J-K)$ colour the spectral type of the companion is L5. Plotted here are the UVEX and UKIDSS photometry with error bars, the WHT spectrum of V12b (red) and a Koester DA white dwarf atmosphere model with $T_{\rm eff}$ = 13 kK and log (*g*) = 8.0 (blue).

sdO/sdB stars without a companion, and no UV-excess white dwarfs are clear debris disc candidates.

3.4 UV-excess sources in the Wide-field Infrared Survey data

The release of the all-sky *WISE* catalogue (Cutri et al. 2012) contains all sky data in four MIR bands centred at 3.4, 4.6, 12 and 22µm. There are nine classified UV-excess sources with a *WISE* match, one classified as DA white dwarf, one classified as cataclysmic variable, one classified as DA+dM, one classified as T Tauri star, three classified as sdB stars and two classified as QSOs in V12b. The QSOs and four new QSO candidates are discussed in Section 4. The SEDs of the sources classified as DA+dM (UVEXJ2122+5526), DA (UVEXJ2034+4110; ccd-flag ‘H’ for $W3$), sdB+F (UVEXJ0421+4651; $W3$ and $W4$ are upper limits) and sdB (UVEXJ0328+5035) in V12b are already shown in Fig. 7–11. The SEDs of objects of other types, classified in V12b, with a match in *WISE* are shown in Fig. 13. The two unclassified UV-excess sources (UVEXJ2039+3647 and UVEXJ0009+6514) at $(W2-W3)\sim5.5$ show a strong excess in the $W3$-band (UVEXJ0009+6514 has ccd-flag ‘H’ in $W2$). From their SEDs and position in the *WISE* colour–colour diagram, these two sources are candidate luminous infrared galaxies (LIRGs)/starburst Sbc (fig. 12 of Wright et al. 2008). The four remaining sources are DA+dM or sdB/sdO+MS candidates.

4 CANDIDATE QSOs SELECTED FROM UVEX AND *WISE*

Since the release of the all-sky *WISE* catalogue, the data have been used to select QSOs (Bond et al. 2012; Stern et al. 2012; Wu et al. 2012; Scaringi et al. 2013; Yanxia et al. 2013). The IR-excess of the QSOs in *WISE* is probably due to optically thick material surrounding most QSOs (Roseboom et al. 2013). In Fig. 5, there are six UV-excess sources at the QSO location in the *WISE* colour–colour diagram $[2.5 < (W2-W3) < 4.5$

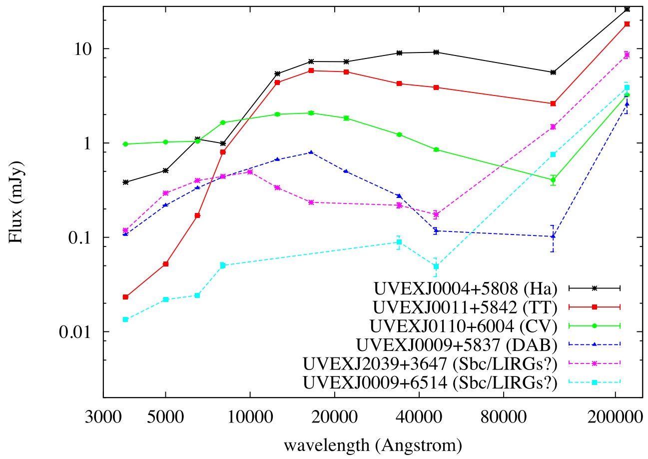

Figure 13. The SEDs of the UV-excess sources classified in V12b with a match in *WISE* and the two unclassified sources at $(W2 - W3) \sim 5.5$ which are candidate starburst Sbc/LIRGs (dashed lines).

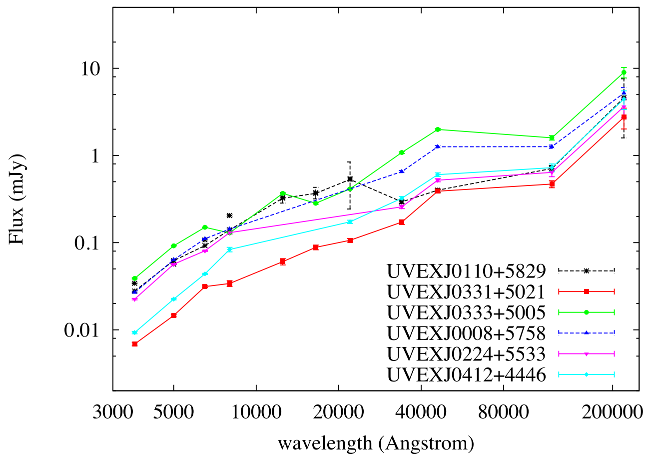

Figure 14. The SEDs of the two classified QSOs of V12b (dashed lines) and the four new candidate QSOs from *WISE* (solid lines).

and $0.6 < (W1 - W2) < 1.7$; see fig. 12 of Wright et al. 2008]. Two of these sources (UVEXJ0008+5758 and UVEXJ0110+5829) were already spectroscopically classified as QSOs in V12b. For UVEXJ0110+5829 $W4$ is an upper limit, the other candidate QSOs have ‘good’ photometry in all *WISE* bands. All six candidate QSOs have similar UVEX colours $(g - r) \sim 0.8$ and $(U - g) \sim -0.2$. In V12a these six sources were selected in g versus $(U - g)$ and not in g versus $(g - r)$ (selection flags ‘515’ and ‘514’) and they are all at Galactic latitude $-5° < b < -4°$ and Galactic longitude $117° > l > 157°$. This might be due to the warp and flare of the Milky Way at this latitude and longitude (Cabrera-Lavers et al. 2007). The effects of the shape are different at different lines of sight, the height of the disc is smaller at some directions and therefore QSOs may be picked-up by UV-excess surveys. The two brightest candidate QSOs have a match in 2MASS, and three of the candidate QSOs have a match in UKIDSS. The SEDs of the two QSOs and new candidate QSOs are shown in Fig. 14. The characteristics of the six UV-excess candidate QSOs are summarized in Table 2.

5 DISCUSSION AND CONCLUSIONS

There are 46 white dwarfs with an IR match in UKIDSS and 3 with a match in 2MASS. Seventeen sources in the $(g - r) < 0.2$ sample turn out to be single white dwarfs. These white dwarfs have bright UVEX g-band magnitudes, have in general a higher $T_{\rm eff}$ and are more reddened compared to the candidate DA+dM sources in the UV-excess candidate white dwarf sample.

In the $(g - r) < 0.2$ sample there are 24 DA+dM candidates, which is a fraction of 2 per cent of the complete UV-excess candidate white dwarf sample. This fraction given here is a lower limit, since the fraction of white dwarfs with a companion is higher for the brighter UV-excess sources (see Fig. 1 and 2). If only UV-excess candidate white dwarfs brighter than $g < 20$ are considered, the fraction of white dwarfs with a companion is 4 per cent. If we compare this result to other studies, the DA+dM fraction is in the range 6–22 per cent (Farihi et al. 2005; Debes et al. 2011b). The presence of an M dwarf has a strong influence on the optical colours for the cooler white dwarfs. Due to the contribution of the M dwarf the colours of the most DA+dM sources are redder than $(g - r) > 0.2$. An unreddened DA+M4V has $(g - r) = 0.2$ for a $T_{\rm eff} \sim 28$ kK white dwarf (fig. 1 of Rebassa-Mansergas et al. 2012; fig. 2 of Augusteijn et al. 2008), while a single DA white dwarf with $T_{\rm eff} = 28$ kK is $(g - r) = -0.185$. The effects on the UV and optical spectrum due to the presence of a debris discs around white dwarfs is negligible (Zabot, Kanaan & Cid Fernandes 2009).

There are seven candidates for white dwarfs with a companion later than type M6V in the UV-excess candidate white dwarf sample. These sources are all brighter than $g < 20$ and the white dwarfs all have an effective temperature lower than $T_{\rm eff} < 20$ kK. This number is in agreement with the WD+BD fractions of other studies (Farihi et al. 2005; Debes et al. 2011b).

No convincing debris disc candidates were found. If the expected rate of white dwarfs with a dust/debris disc would be ∼1 per cent (Girven et al. 2011), there would be ∼4 of them brighter than $g < 20$ in the UV-excess catalogue. Additionally, the IR-excess of one source (UVEXJ0328+5035) can be fully explained by a reddened sdB spectrum without the need for a low-mass companion.

There are two known QSOs and four UV-excess candidate QSOs in *WISE*. Since the number of QSOs from the *WISE* cross-matching (6 of 2170) is much smaller than the fraction of QSOs found in the spectroscopic follow-up of UV-excess sources in V12b (2 of 132), there might be some more QSOs in the UV-excess catalogue. However, the QSOs at $|b| < 5$ are expected to be clustered at specific lines of sight where absorption is not so strong. The fact that all known UVEX QSOs have a *WISE* match shows that adding *WISE* data is a good additional selection criteria. A list of UV-excess candidate QSOs is given in Table 2. The UVEX colours of these candidate QSOs are at $0.65 < (g - r) < 1.10$ and $-0.21 < (U - g) < -0.03$ (Fig. 1 and 2), which are the colour ranges of known QSOs.

ACKNOWLEDGEMENTS

This paper makes use of data collected at the Isaac Newton Telescope, operated on the island of La Palma by the Isaac Newton Group in the Spanish Observatorio del Roque de los Muchachos of the Instítuto de Astrofísica de Canarias. The observations were processed by the Cambridge Astronomy Survey Unit (CASU) at the Institute of Astronomy, University of Cambridge. Hectospec observations shown in this paper were obtained at the MMT Observatory, a joint facility of the University of Arizona and the Smithsonian Institution. We gratefully acknowledge the IPHAS consortium for making available the IPHAS-IDR data. The WHT/ISIS spectra were reduced in V12b using Image Reduction and Analysis Facility (IRAF). IRAF is distributed by the National Optical Astronomy Observatory, which is operated by the Association of Universities for

Table 2. UV-excess candidate QSOs from *WISE*.

Name	l	b	Field	Selection	$\langle r\rangle$	$\langle g\rangle$	$\langle U\rangle$	$W1$	$W2$	$W3$	$W4$
UVEXJ000848.64+575832.7	117.3	−4.43	48	515	18.625	19.494	19.402	14.189	12.837	10.016	8.126
UVEXJ033309.70+500541.8	147.6	−4.86	1243	515	18.296	19.093	18.999	13.642	12.341	9.763	7.532
UVEXJ033113.88+502156.9	147.2	−4.82	1243	515	19.996	21.093	20.880	15.637	14.111	11.089	8.817
UVEXJ022445.84+553325.9	135.9	−4.94	810	514	18.971	19.620	19.593	15.200	13.797	10.754	8.516
UVEXJ041204.47+444629.6	156.1	−4.80	1570	515	19.631	20.623	20.552	14.954	13.637	10.618	8.298
UVEXJ011037.91+582928.1	125.4	−4.29	404	515	18.821	19.518	19.360	15.056	14.083	10.643	8.262

Research in Astronomy (AURA) under cooperative agreement with the National Science Foundation. The authors would like to thank Detlev Koester for making available the white dwarf atmosphere model spectra. The TheoSSA service (http://dc.g-vo.org/theossa), used to retrieve theoretical sdO and sdB spectra for this paper, was constructed as part of the activities of the German Astrophysical Virtual Observatory. This research has made use of the Simbad data base and the VizieR catalogue access tool, operated at CDS, Strasbourg, France. The original description of the VizieR service was published in A&AS 143, 23. This publication makes use of data products from the *Wide-field Infrared Survey Explorer* (*WISE*), which is a joint project of the University of California, Los Angeles, and the Jet Propulsion Laboratory/California Institute of Technology, funded by the National Aeronautics and Space Administration. This publication makes use of data products from the Two Micron All Sky Survey (2MASS), which is a joint project of the University of Massachusetts and the Infrared Processing and Analysis Center/California Institute of Technology, funded by the National Aeronautics and Space Administration and the National Science Foundation. This work is based in part on data obtained as part of the UKIRT Infrared Deep Sky Survey (UKIDSS). We want to credit the efforts of the teams which built WFCAM, processed the data, and implemented the UKIDSS surveys. The UKIDSS project is defined in Lawrence et al. (2007). UKIDSS uses the UKIRT Wide Field Camera (WFCAM; Casali et al. 2007). The photometric system is described in Hewett et al. (2006), and the calibration is described in Hodgkin et al. (2009). The pipeline processing and science archive are described in Irwin et al. (in preparation) and Hambly et al. (2008). This paper uses data obtained by the Sloan Digital Sky Survey (SDSS) DR8 (Aihara et al. 2011a). The Sloan Digital Sky Survey III (Eisenstein et al. 2011) is an extension of the SDSS-I and II projects (York et al. 2000). It uses the dedicated 2.5-m wide-field Sloan Foundation Telescope (Gunn et al. 2006) at Apache Point Observatory (APO). Funding for the Sloan Digital Sky Survey has been provided by the Alfred P. Sloan Foundation, the Participating Institutions, the National Aeronautics and Space Administration, the National Science Foundation, the US Department of Energy, the Japanese Monbukagakusho and the Max Planck Society. The SDSS website is http://www.sdss.org/. The SDSS is managed by the Astrophysical Research Consortium (ARC) for the Participating Institutions. KV is supported by a NWO-EW grant 614.000.601 to PJG and by NOVA.

REFERENCES

Adelman-McCarthy J. K. et al., 2011, VizieR On-line Data Catalog, 2306, 0
Aihara H. et al., 2011, ApJS, 193, 29
Augusteijn T., Greimel R., van den Besselaar E. J. M., Groot P. J., Morales-Rueda L., 2008, A&A, 486, 843
Barber S. D., Patterson A. J., Kilic L., Leggett S. K., Dufour P., Bloom J. S., Starr D. L., 2012, ApJ, 760, 26
Barentsen G. et al., 2011, MNRAS, 415, 103
Beuermann K., 2006, A&A, 460, 783
Blanton M. R., Roweis S., 2007, AJ, 133, 734
Bond N. A. et al., 2012, ApJ, 750, L18
Brinkworth C. S., Gänsicke B. T., Girven J. M., Hoard D. W., Marsh T. R., Parsons S. G., Koester D., 2012, ApJ, 750, 86
Brinkworth C. S., Gänsicke B. T., Marsh T. R., Hoard D. W., Tappert C., 2009, ApJ, 696, 1402
Cabrera-Lavers A., Bilir S., Ak S., Yaz E., Lopez-Corredoira M., 2007, A&A, 464, 565
Cardelli J. A., Clayton G. C., Mathis J. S., 1989, ApJ, 345, 245
Casali M. et al., 2007, A&A, 467, 777
Corradi R. L. M. et al., 2010, A&A, 509, 41
Corradi R. L. M. et al., 2011, MNRAS, 410, 1349
Cutri R. M. et al., 2003, VizieR On-line Data Catalog, 2246, 0
Cutri R. M. et al., 2012, VizieR On-line Data Catalog, 2311, 0
Deacon N. R. et al., 2009, MNRAS, 397, 1685
Debes J. H., Hoard D. W., Kilic M., Wachter S., Leisawitz D. T., Cohen M., Kirkpatrick J. D., Griffith R. L., 2011a, ApJ, 729, 4
Debes J. H., Hoard D. W., Wachter S., Leisawitz D. T., Cohen M., 2011b, ApJS, 197, 38
Debes J. H., Sigurdsson S., 2002, ApJ, 572, 556
Debes J. H., Walsh K. J., Stark C., 2012, ApJ, 747, 148
Drew J. E. et al., 2005, MNRAS, 362, 753 (D05)
Dufour P., Kilic M., Fontaine G., Bergeron P., Melis C., Bochanski J., 2012, ApJ, 749, 6
Eisenstein D. J. et al., 2011, AJ, 142, 72
Farihi J., Becklin E. E., Zuckerman B., 2005, ApJS, 161, 394
Farihi J., Gänsicke B. T., Steele P. R., Girven J., Burleigh M. R., Breedt E., Koester D., 2012, MNRAS, 421, 1635
Gänsicke B. T., 2011, in AIP Conf. Proc. Vol. 1331. Planetary Systems beyond the Main Sequence. Am. Inst. Phys., New York, p. 211
Gänsicke B. T., Koester D., Farihi J., Girven J., Parsons S. G., Breedt E., 2012, MNRAS, 424, 333
Gänsicke B. T., Koester D., Marsh T. R., Rebassa-Mansergas A., Southworth J., 2008, MNRAS, 391, L103
Gänsicke B. T., Marsh T. R., Southworth J., 2007, MNRAS, 380, L35
Girven J., Gänsicke B. T., Steeghs D., Koester D., 2011, MNRAS, 417, 1210
González-Solares E. A. et al., 2008, MNRAS, 388, 89
Greiss S. et al., 2012, AJ, 144, 24
Groot P. J. et al., 2009, MNRAS, 399, 323
Gunn J. E. et al., 2006, AJ, 131, 2332
Hales A. S., Barlow M. J., Drew J. E., Unruh Y. C., Greimel R., Irwin M. J., González-Solares E., 2009, ApJ, 695, 75
Hambly N. C. et al., 2008, MNRAS, 384, 637
Heller R., Homeier D., Dreizler S., Oestensen R., 2009, A&A, 496, 191
Hewett P. C., Warren S. J., Leggett S. K., Hodgkin S. T., 2006, MNRAS, 367, 454
Hoard D. W., Debes J. H., Wachter S., Leisawitz D. T., Cohen M., 2011, AAS Meeting, 217, 33309
Hoard D. W., Wachter S., Sturch L. K., Widhalm A. M., Weiler K. P., Pretorius M. L., Wellhouse J. W., Gibiansky M., 2007, AJ, 134, 26
Hodgkin S. T., Irwin M. J., Hewett P. C., Warren S. J., 2009, MNRAS, 394, 675
Jura M., 2003, ApJ, 584, L91
Kilic M., Patterson A. J., Barber S., Leggett S. K., Dufour P., 2012, MNRAS, 419, L59

Koester D., 2009, A&A, 498, 517
Koester D. et al., 2001, A&A, 378, 556
Koester D., Wilken D., 2006, A&A, 453, 1051
Kupfer T. et al., 2013, preprint (arXiv:1308.2447)
Lawrence A. et al., 2007, MNRAS, 379, 1599
Lawrence A. et al., 2012, VizieR On-line Data Catalog, 2314, 0
Leggett S. K. et al., 2002, ApJ, 564, 452
Lucas P. W. et al., 2008, MNRAS, 391, 136
Pickles A. J., 1998, PASP, 110, 863
Rebassa-Mansergas A., Gänsicke B. T., Schreiber M. R., Koester D., Rodríguez-Gil P., 2010, MNRAS, 402, 620
Rebassa-Mansergas A., Nebot Gómez-Morán A., Schreiber M. R., Gänsicke B. T., Schwope A., Gallardo J., Koester D., 2012, MNRAS, 419, 806
Reid I. N., Burgasser A. J., Cruz K. L., Kirkpatrick J. D., Gizis J. E., 2001, AJ, 121, 1710
Ringat E., 2012, in ASP Conf. Ser. Vol. 452, Fifth Meeting on Hot Subdwarf Stars and Related Objects. Astron. Soc. Pac., San Francisco, p. 99
Roseboom I. G., Lawrence A., Elvis M., Petty S., Shen Y., Hao H., 2013, MNRAS, 429, 1494
Scaringi S., Groot P. J., Verbeek K., Greiss S., Knigge C., Koerding E., 2013, MNRAS, 428, 2207
Silvestri N. M. et al., 2006, AJ, 131, 1674
Skrutskie M. F. et al., 2006, AJ, 131, 1163
Steele P. R., Burleigh M. R., Dobbie P. D., Jameson R. F., Barstow M. A., Satterthwaite R. P., 2011, MNRAS, 416, 2768
Stern D. et al., 2012, ApJ, 753, 30
Verbeek K. et al., 2012a, MNRAS, 420, 1115 (V12a)
Verbeek K. et al., 2012b, MNRAS, 426, 1235 (V12b)
Wachter S., Hoard D. W., Hansen K. H., Wilcox R. E., Taylor H. M., Finkelstein S. L., 2003, ApJ, 586, 1356
Wesson R. et al., 2008, ApJ, 688, L21
Witham A. R., Knigge C., Drew J. E., Greimel R., Steeghs D., Gänsicke B. T., Groot P. J., Mampaso A., 2008, MNRAS, 384, 1277
Wright N. J. et al., 2008, MNRAS, 390, 929
Wright N. J., Drake J. J., Drew J. E., Guarcello Mario G., Gutermuth R. A., Hora J. L., Kraemer K. E., 2012, ApJ, 746, L21
Wu X. B., Hao G., Jia Z., Zhang Y., Peng N., 2012, AJ, 144, 49
Yanxia Z., He M., Nanbo P., Yongheng Z., Xue-bing W., 2013, preprint (arXiv:1305.5023)
York D. G. et al., 2000, AJ, 120, 1579
Zabot A., Kanaan A., Cid Fernandes R., 2009, ApJ, 704, L93
Zuckerman B., Becklin E. E., 1987, Nat, 330, 138

APPENDIX A: UV-EXCESS SOURCES WITH AN IR-EXCESS

Table A1. UV-excess candidate white dwarfs with a match in UKIDSS (46) or 2MASS (3). Here 'Selec' is column 20 of the UV-excess catalogue of V12a, 'Reg.' is the region in the $(J - H)$ versus $(H - K)$ colour–colour diagram and 'Fit' shows the fitting results: (i) $T_{\rm eff}$ (kK) of the white dwarf, (ii) $E(B - V)$ and (iii) the spectral type of companion (M-type determined by fitting the photometry, or BD determined from the resulting $(J - K)$ colour).

No	Name	l	b	Field	Selec	r	g	U	(J)	(H)	(K)	Reg.	Fit	V12b
1	UVEXJ183141.67+002201.5	31.00431	4.55953	4088	1543	17.266	17.351	16.970	17.500	17.499	17.663	1	13,0.1	
2	UVEXJ183605.84+014117.8	32.68689	4.18264	4112	1028	18.651	18.717	17.978	17.922	17.346	17.186	2	22,0.2,M4V	
3	UVEXJ184610.80+022032.4	34.41846	2.23713	4183	1028	18.158	18.253	17.933	17.866	17.532	17.326	3	14,0.2,L2	
4	UVEXJ184725.16−011039.4	31.42575	0.35696	4197	1543	16.992	17.208	16.804	16.700	16.592	16.764	1	17,0.3	
5	UVEXJ184736.88-004413.1	31.84015	0.51452	4197	1543	20.435	20.594	20.508	19.457	18.016	17.403	2	13,0.3,M4V	
6	UVEXJ185519.35+114741.5	43.88889	4.49896	4294	1543	18.057	18.155	17.821	18.000	18.024	18.076	1	15,0.2	
7	UVEXJ185710.76+043917.5	37.72853	0.84714	4338	1543	19.266	19.290	18.976	17.930	16.512	15.469	2	22,0.1,M5V	
8	UVEXJ185941.43+013954.0	35.35485	−1.07596	4404	1543	18.133	18.180	17.853	18.325	17.949	17.423	3	13,0.1,L7	
9	UVEXJ190129.69+075854.1	41.17849	1.41266	4414	1543	17.800	17.815	17.046	18.089	17.842	17.874	1	24,0.2	
10	UVEXJ190257.79+113618.9	44.56953	2.74590	4469	1028	18.495	18.508	18.009	17.524	16.889	16.710	2	13,0.0,M6V	
11	UVEXJ190310.08+140658.9	46.83175	3.84480	4453	1028	17.595	17.667	16.743	17.621	17.578	17.524	1	35,0.3	
12	UVEXJ191001.10+055542.5	40.32597	−1.40915	4591	1543	18.154	18.209	17.585	17.926	17.526	17.170	3	20,0.2,L5	
13	UVEXJ202432.88+412338.9	79.33309	2.15868	5889	1543	17.351	17.207	16.286	17.835	18.387	19.690	1	22,0.0	
14	UVEXJ202654.69+430152.1	80.92379	2.74656	5923	1028	21.309	21.491	21.140	19.594	18.617	18.038	2	11,0.1,M6V	
15	UVEXJ202659.21+411644.1	79.50370	1.71848	5916	1028	17.175	17.092	16.389	16.323	15.996	15.707	3	17,0.0,L3	DA
16	UVEXJ202701.05+405909.2	79.26842	1.54359	5916	1028	20.996	21.067	20.797	19.607	18.666	17.982	2	14,0.2,M2V	
17	UVEXJ202800.47+405620.0	79.33903	1.36420	5939	1028	16.328	16.177	17.676	16.833	16.898	16.994	1	14,0.1	DA
18	UVEXJ202940.45+424613.7	81.00707	2.18354	5947	1028	19.839	19.939	19.418	17.505	16.758	16.287	2	50,0.2,M2V	
19	UVEXJ203238.52+411339.4	80.08644	0.82801	6010	1543	19.446	19.295	18.520	18.110	16.700	16.004	2	50,0.0,M6V	DA
20	UVEXJ203326.92+410959.9	80.12765	0.66975	6010	1543	20.967	21.135	20.775	18.406	16.892	16.001	2	13,0.1,M6V	
21	UVEXJ203614.30+392309.8	79.02005	−0.82249	6036	1029	19.582	19.776	19.192	17.184	16.662	16.443	2	45,0.4,M2V	DA+dM
22	UVEXJ204154.36+393201.4	79.80276	−1.60107	6118	1543	19.196	19.360	19.019	18.306	17.646	17.503	2	14,0.2,M4V	
23	UVEXJ204203.59+413343.1	81.42044	−0.37688	6112	1543	21.044	21.199	20.485	19.370	17.779	17.168	2	30,0.4,M0V	
24	UVEXJ204212.01+402706.7	80.56161	−1.08086	6111	1543	18.828	19.018	18.172	16.703	16.179	15.910	2	75,0.5,M6V	
25	UVEXJ204229.67+384058.0	79.20167	−2.21444	6108	1543	19.194	19.344	18.904	19.079	18.707	18.516	3	16,0.2,L2	
26	UVEXJ204401.03+403014.5	80.81605	−1.32043	6143	1543	15.436	15.419	15.044	15.616	15.667	15.736	1	14,0.1	
27	UVEXJ204502.52+414622.9	81.93084	−0.68385	6145	1543	17.255	17.406	16.741	17.238	17.276	17.317	1	28,0.4	
28	UVEXJ204502.62+385449.5	79.69073	−2.46193	6172	1028	21.678	21.666	21.370	19.553	18.449	18.231	2	30,0.1,M4V	
29	UVEXJ204503.63+435657.2	83.63666	0.66749	6153	1028	19.234	19.171	18.334	18.691	18.013	17.518	2	75,0.1,M5V	
30	UVEXJ204628.29+433237.6	83.47876	0.21540	6176	1543	20.841	20.827	20.039	18.999	18.078	17.656	2	20,0.1,M2V	
31	UVEXJ204720.64+444310.3	84.49330	0.82997	6196	1543	18.436	18.572	18.181	17.001	16.279	16.061	2	15,0.2,M2V	
32	UVEXJ204751.27+442920.1	84.37091	0.61442	6196	1028	20.004	19.960	19.457	17.952	16.947	16.365	2	14,0.0,M6V	DA
33	UVEXJ204804.01+421720.8	82.68492	−0.79916	6209	1543	19.721	19.677	19.124	19.431	18.456	18.161	2	14,0.0,M6V	
34	UVEXJ204830.05+423250.4	82.93598	−0.69880	6188	1031	21.198	21.121	20.907	19.172	18.430	17.939	2	13,0.1,M0V	
35	UVEXJ204856.21+444455.0	84.69394	0.62843	6196	1028	18.638	18.513	17.832	18.898	18.502	17.962	3	16,0.0,L7	
36	UVEXJ204914.51+421623.0	82.80950	−0.97798	6209	1028	16.610	16.784	16.434	16.608	16.554	16.677	1	14,0.2	
37	UVEXJ204938.33+432018.0	83.68083	−0.36073	6199	1543	19.137	19.328	18.962	18.906	18.721	18.555	3	11,0.1,M8V	

Table A1 – *continued*

No	Name	l	b	Field	Selec	r	g	U	(J)	(H)	(K)	Reg.	Fit	V12b
38	UVEXJ205037.81+424618.9	83.35761	−0.85988	6220	1543	15.793	15.750	15.132	16.198	16.242	16.277	1	15,0.0	DA
39	UVEXJ205148.13+442408.8	84.75023	0.01441	6219	1028	17.806	17.707	16.905	18.333	18.499	18.452	1	18,0.0	DA
40	UVEXJ205636.98+434541.6	84.81618	−1.05975	6293	1028	19.694	19.666	19.196	19.342	18.285	17.752	2	13,0.0,M6V	
41	UVEXJ210112.02+452020.7	86.54346	−0.64434	6355	519	16.131	16.272	17.069	16.114	16.056	16.037	1	14,0.8	
42	UVEXJ210248.44+475058.9	88.60784	0.81096	6341	1543	18.313	18.300	17.879	18.228	17.726	17.456	2	80,0.1,L5	DA
43	UVEXJ210454.41+460041.9	87.47634	−0.68123	6365	1543	18.778	18.738	17.856	18.762	18.334	18.196	1	24,0.1	DB
44	UVEXJ223634.77+591907.8	106.47749	0.82554	7139	1028	17.752	17.675	16.937	18.041	18.032	18.054	1	17,0.0	DA
45	UVEXJ224338.89+550318.5	105.25732	−3.37032	7188	519	16.501	16.547	15.781	16.521	16.546	16.680	1	24,0.2	
46	UVEXJ224436.07+544812.6	105.25981	−3.65677	7188	518	15.640	15.780	15.359	15.319	15.163	15.129	1	16,0.2	
47	UVEXJ032855.25+503529.8	146.76969	−4.84547	1224	519	14.078	14.205	13.591	14.121	14.091	14.263	1	sdO/sdB	sdB
48	UVEXJ185740.07+075557.3	40.70227	2.23345	4346	1028	18.821	19.024	18.656	15.540	14.402	13.833	2	DA+M/L5	DA
49	UVEXJ203411.72+411020.3	80.21601	0.56034	6010	1543	20.446	20.426	19.875	14.512	11.915	10.767	2	DA+M/L8	DA

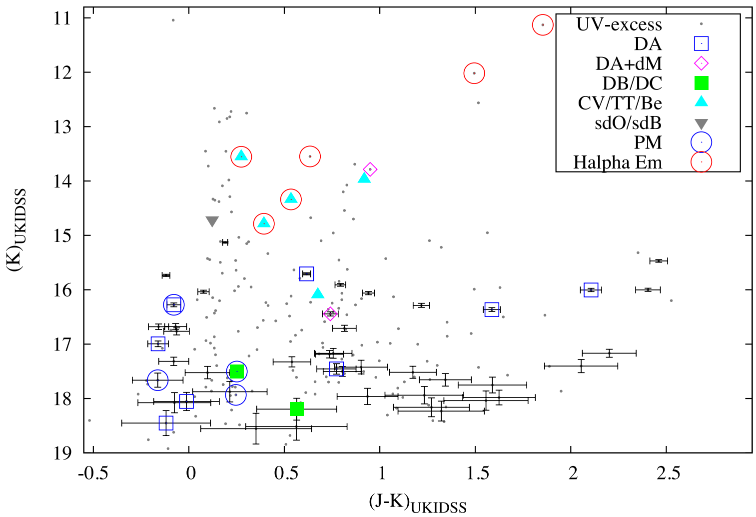

Figure A1. The K versus $(J - K)$ colour–magnitude diagram with the UKIDSS-GPS matches. UV-excess sources spectroscopically classified in V12b are overplotted with different symbols, UV-excess candidate white dwarfs with $(g - r) < 0.2$ are plotted with error bars and other UV-excess sources are plotted with dots.

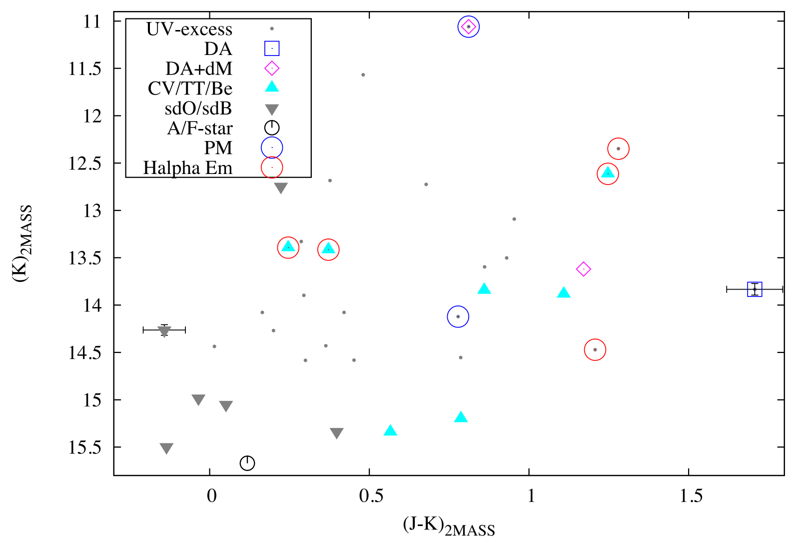

Figure A2. K versus $(J - K)$ colour–magnitude diagram with the UV-excess matches in 2MASS. Classified sources are labelled with different symbols, UV-excess candidate white dwarfs are plotted with error bars and other UV-excess sources are plotted with dots. There is one more match at $(J - K) = 3.7$, $K = 10.8$, classified as DA white dwarf in V12b, not visible in this figure.

This paper has been typeset from a TEX/LATEX file prepared by the author.